Journal of
Applied Remote Sensing

RemoteSensing.SPIEDigitalLibrary.org

Light detection and ranging and hyperspectral data for estimation of forest biomass: a review

Qixia Man
Pinliang Dong
Huadong Guo
Guang Liu
Runhe Shi

SPIE.

REVIEW

Light detection and ranging and hyperspectral data for estimation of forest biomass: a review

Qixia Man,[a,b,c] Pinliang Dong,[d,*] Huadong Guo,[b,c] Guang Liu,[c] and Runhe Shi[a,b]

[a]East China Normal University, Key Laboratory of Geographic Information Science (Ministry of Educating), No. 500 Dongchuan Road, Minhang District, Shanghai 200241, China
[b]East China Normal University and Institute of Remote Sensing and Digital Earth (RADI), Joint Laboratory for Environmental Remote Sensing and Data Assimilation, No. 500 Dongchuan Road, Minhang District, Shanghai 200241, China
[c]Chinese Academy of Sciences, Institute of Remote Sensing and Digital Earth (RADI), Key Laboratory of Digital Earth, No. 9 Dengzhuang South Road, Haidian District, Beijing 100094, China
[d]University of North Texas, Department of Geography, 1155 Union Circle #305279, Denton, Texas 76203, United States

Abstract. Forests are one of the most important sinks for carbon. Estimating the amount of carbon stored in forests is a major task for understanding the global carbon cycle. From local to global scales, remote sensing has been extensively used for forest biomass estimation. With the availability of multisensor image data, fusion has become a valuable method in remote sensing applications. Light detection and ranging (LiDAR) can provide information on the vertical structure of forests, whereas hyperspectral images can provide detailed spectral information of forests. Effective fusion of LiDAR and hyperspectral data is expected to help extract important biophysical parameters of forests. However, it is still unclear as to how forest biophysical and biochemical attributes derived from hyperspectral data relate to structural attributes derived from LiDAR data. A summary of previous research on LiDAR-hyperspectral fusion for forest biomass estimation is valuable for further improvement of biomass estimation methods. A review on the status of hyperspectral data, LiDAR data, and the fusion of these two data sources for forest biomass estimation in the last decade is provided. Some future research topics and major challenges are also discussed. [DOI: 10.1117/1.JRS.8.081598]

Keywords: light detection and ranging; hyperspectral; data fusion; aboveground biomass.

Paper 14411V received Jul. 15, 2014; accepted for publication Nov. 13, 2014; published online Dec. 18, 2014.

1 Introduction

The complex structure and diverse material resources of a forest make it a perfect resource pool and biological gene bank for nature. Forest ecosystems have an irreplaceable role in improving the ecological environment and maintaining ecological balance. In addition, forest ecosystems are also an important component of the carbon cycle, in which forest ecosystems account for 80% of the aboveground carbon stocks and 40% of the underground carbon stocks.[1,2] In recent years, carbon sequestration has been a hot topic in climate change studies[3] and carbon balance estimation.[4] From local to global scales, it is of increasing importance to quantify forest carbon exchange and stocks because of international policies to reduce greenhouse gases, such as the United Nations Framework Convention on Climate Change (UNFCCC),[5] the Kyoto protocol,[4] and the program for reducing emissions from deforestation and forest degradation (REDD).[5–9]

*Address all correspondence to: Pinliang Dong, E-mail: pdong@unt.edu

Forest biomass is one of the main biophysical parameters that describe the carbon content of the forest.[10,11] Therefore, accurate estimation and assessment of forest biomass are important to quantify terrestrial carbon, control greenhouse gases, keep forest sustainably managed, and make policies which can reduce CO_2 mission.[11,12] Field measurements are the traditional methods for forest biomass estimation. However, it is destructive, labor intensive, costly, time consuming, and sometimes inapplicable due to poor accessibility.[13] Remote sensing has been frequently used as a practical and economical means for forest biochemical and biophysical parameters estimation, and a primary source for forest biomass estimation.[14] At local to sub-regional scales, intermediate and fine resolution remote sensors have been used for biomass estimation,[15] such as Landsat ETM+,[16] SPOT,[17] and WorldView-2.[18] At regional to national scales, coarse resolution sensors were used such as National Oceanic and Atmospheric Administration (NOAA), Advanced Very High Resolution Radiometer (AVHRR),[19] and Moderate Resolution Imaging Spectroradiometer (MODIS).[20]

Hyperspectral sensors acquire hundreds of narrow bands of the electromagnetic spectrum from visible to short-wave infrared wavelengths which could provide detailed and continuous spectral information of forests,[21] whereas light detection and ranging (LiDAR) has been known as a vital method for characterizing forest vertical structures, including height, volume, and biomass. With the availability of multisensor image data, effective fusion of the two complementary data sources can improve the estimation of forest biomass and other forest structure parameters.[22–25]

Many previous papers have reviewed forest biomass estimation using remote sensing. Lu[14] reviewed the potential and challenge of remote sensing-based biomass estimation and pointed out that biomass estimation is still a challenging task, especially for areas with complex forest structure and environmental conditions. Koch[3] reviewed the status and future of three remote sensing technologies (LiDAR, synthetic aperture radar, and hyperspectral remote sensing) for forest biomass estimation. Treitz and Howarth[26] published a review on hyperspectral remote sensing for estimation of forest biophysical parameters. Govender et al.[27] provided a review of hyperspectral remote sensing and its application in vegetation and water resource studies. Adam et al.[28] reviewed multispectral and hyperspectral remote sensing for identification and mapping of wetland vegetation. Lim et al.[29] reviewed the recent research progresses of LiDAR on forest structure extraction, including canopy height, volume, and biomass. Van Leeuwen and Nieuwenhuis (2010)[30] reviewed the methods and challenges in forest inventory using LiDAR. Frolking et al.[31] reviewed the impacts of forest disturbance and recovery on aboveground biomass (AGB) and canopy structure in the context of space-borne remote sensing. Since the review by Koch,[3] many papers, which will be included in this review, have been published on the fusion of hyperspectral and LiDAR data for forest biomass estimation.

Although research on biomass estimation using remote sensing has been investigated in the past decades, a comprehensive review on the fusion of LiDAR and hyperspectral data for forest biomass estimation is still lacking. It is unclear as to how forest biophysical and biochemical parameters derived from hyperspectral data relate to the structural attributes from LiDAR data. Many studies have involved the fusion of hyperspectral and LiDAR data in forest biomass application, which makes it possible to provide an overview of the techniques that have been used and to identify the aspects that still need further investigation. This review consists of the following six major parts: (1) overview of LiDAR and hyperspectral remote sensing systems and concepts of image fusion; (2) AGB estimation using LiDAR data; (3) AGB estimation using hyperspectral data; (4) fusion of LiDAR and hyperspectral data for biomass estimation; (5) discussion of current challenges and research needs; and (6) general conclusions.

2 Definitions

2.1 *Overview of LiDAR Systems*

LiDAR is an active remote sensing technology that determines distances based on the speed of light and the time required for an emitted laser to reach a target object. It can simultaneously capture vertical and horizontal forest structure and terrain morphology with high accuracy.[32] The components of LiDAR systems includes laser and scanning subsystems, a global position

system, and an inertial measurement unit. The basic ranging principle can be expressed with the following equation:

$$R = ct/2, \tag{1}$$

where R represents the distance from the sensor to the object; c is the speed of light; and t is the round-trip transmission time from the sensor to the measured target.

Dubayah and Drake[33] summarized three characteristics that can be used to classify LiDAR systems for forestry applications, including: (1) the manner in which the return signal is recorded as either discrete return LiDAR, which typically includes the first, last, and several intermediate returns, versus the full-waveform LiDAR, which characterizes the returned energy in a continuous manner;[34] (2) footprint size—small (a few centimeters) or large (tens of meters); and (3) sampling rate and scanning pattern.

2.2 *Overview of Hyperspectral Systems*

Hyperspectral remote sensing is a technology that acquires hundreds of narrow continuous spectral bands between 400 and 2500 nm, throughout the visible (400 to 700 nm), near-infrared (700 to 1000 nm), and short-wave infrared (1000 to 2500 nm) sections of the electromagnetic spectrum.[35] It is also known as imaging spectroscopy or imaging spectrometry.

2.3 *Methods of Forest AGB Estimation*

Biomass is the dry weight of living and dead organisms.[36,37] In forests, aboveground living biomass mainly includes the wood of canopy trees, vine, epiphyte, canopy leaf, understory, and groundcover biomass and would exclude all aboveground dead material.[38]

In remote sensing applications, biomass normally refers to the AGB. Measurements of biomass can be divided into direct and indirect methods. As for direct estimations, based on the relationship between remote sensing response and the biomass, AGB can be estimated with different methods, such as multiple regression analysis, K nearest neighbor classification, neural network, and statistical ensemble methods.[3,39–43] For indirect methods, the mean tree height or diameter at breast height are derived from remote sensing images.[44–47] Using these parameters, biomass is obtained through allometric equations.[48] For individual trees, biomass is added to get the AGB for the whole plot.

2.4 *Concepts of Image Fusion*

Image fusion can be defined as the combination of two or more different images into a new image using algorithms.[49] Based on the stage at which fusion occurs, image fusion can be divided into three levels: pixel level; feature level, and decision level.[50,51] (1) Pixel level: After coregistration, a series of raster data layers are directly added to an image which has more abundant and reliable information. Pixel-level fusion is the lowest level of image fusion, in which information synthesis and analysis based on the original information of various images are conducted. Its merit is keeping most of the original information which could provide subtle information, while the shortcomings are mainly reflected in the following four aspects: (a) large amount of information, long processing time, and high cost; (b) because of the uncertainty, insecurity, and instability of the original information, it requires high error correction capability during the fusion process; (c) low anti-interference ability; and (d) the fusion process requires a pixel calibration accuracy. (2) Feature level: Using segmentation procedures, remote sensing images are processed individually using feature extraction to generate unidentified features. The feature extraction processes mainly depend on the image elements such as shape, extent, and neighborhood.[52] The extracted objects from multiple data sources are then fused for further assessment using statistical approaches such as artificial neural networks (ANN).[50] By combining the features of the two datasets, the identification of features is carried out. Feature-level fusion could keep sufficient important information, achieve objective data compression and guarantee a certain accuracy. (3) Decision level: datasets are processed completely separately, and only the final

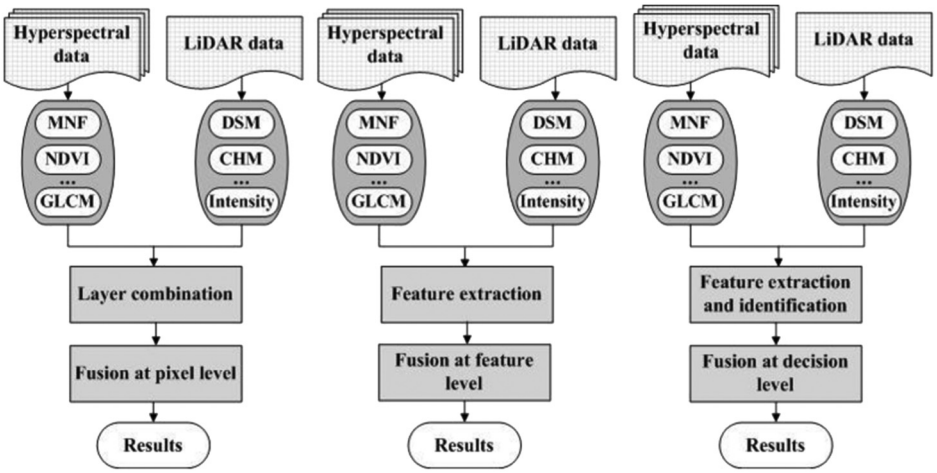

Fig. 1 Levels of image fusion, from left to right: pixel-level, feature level, and decision level (take hyperspectral-LiDAR fusion as an example), MNF: minimum noise fraction; NDVI: normalized difference vegetation index; GLCM: gray level co-occurrence matrix; DSM: digital surface model; CHM: canopy height model.

results are combined in geographic information systems. Apart from the three fusion levels, image fusion can also be applied to various data types, e.g., single sensor and multisensor.[50] Figure 1 shows the three levels of data fusion.

3 ABG Estimation with LiDAR Data

LiDAR technology can provide horizontal and vertical information about the forest canopy which makes it one of the most applicable technologies in forest monitoring. LiDAR data has been used to derive tree height,[53] estimate stem volume,[54] and classify tree species.[55] An overview of LiDAR for forest applications can be found in the papers by Lim et al.,[29] Hyyppä et al.,[56] and Mallet and Bretar[57] These papers reviewed recent research progress on the extraction of canopy height, estimation of ABG, and canopy volume from LiDAR as well as the status of small footprint, multiple point or full-wave LiDAR data for forest applications. Table 1 shows the previous studies of forest biomass estimation using LiDAR data.

Compared with other sensors, Airborne LiDAR data is much more effective for forest biomass estimation.[66] Many studies have described the approaches of biomass estimation from LiDAR data, including single regression between LiDAR-derived height metrics, tree crown delineation and biomass, stochastic simulation and machine learning approaches.[67] There are two levels of forest biomass estimation: individual-tree level and plot-level.[12]

3.1 *Individual Tree Level*

With individual tree level forest biomass estimation, a crown height map (CHM) was produced from raw LiDAR point cloud data; then, individual trees were identified by applying algorithms to locate the maximum heights in CHM, such as local maxima filtering; finally, biomass was calculated by using regression between the tree height and biomass. There were numerous methods for local maxima filtering based on different search window sizes.[67] Popescu[68] identified the crown diameter from a CHM using local maxima filtering and quantified forest biomass by using regression algorithms which included crown width as a parameter. His study managed to explain 93% of the biomass using individual tree metrics. Recently, some researchers have developed advanced methods to identify individual trees. Bortolot and Wynne[69] proposed a new individual tree-based algorithm for forest biomass estimation using small footprint LiDAR data. Kwak et al.[70] proposed a watershed segmentation algorithm to identify individual trees. While biomass

Table 1 Summary of the previous studies of LiDAR-based biomass.

References	Parameters	Regression	Results
Nelson et al.[58]	Average of the three greatest laser heights, mean plot height (all pulses and canopy pulses), distance between the top of canopy and a point 2, 5 or 10 m aboveground	Two logarithmic equations	$R^2 = 0.55$
Means et al.[59]	LiDAR canopy height, quadratic mean canopy height, canopy reflectance sum	Allometric equations on DBH	$R^2 = 0.96$
Lefsky et al.[60]	Max/min canopy height, canopy cover, variability in the upper canopy surface, total volumes of foliage and empty space in canopy	Stepwise multiple regression	$R^2 = 0.86$
Drake et al.[61]	LiDAR canopy height, height of median energy, height /median ratio, ground return ratio	The tropical wet allometric equation	$R^2 = 0.93$
Nelson et al.[62]	Quadratic mean height of pulses in the forest canopy	Parametric linear regression, nonparametric linear regression	$R^2 = 0.66$
Popescu et al.[63]	Average/maximum crown diameter; maximum height	Regression models	$R^2 = 0.82$(Pine), $R^2 = 0.33$(hardwoods)
Zhao et al. 2009[64]	LiDAR-derived canopy height distributions (CHD) canopy height quartile functions (CHQ)	A linear functional model and an equivalent nonlinear model	$R^2 = 0.95$
García et al.[11]	LiDAR height, intensity or height combined with intensity data	A stepwise regression	$R^2 = 0.85$(Pine), $R^2 = 0.70$(Spanish juniper), $R^2 = 0.90$(Holmoak)
Zhao et al.[65]	LiDAR composite metrics	Support vector machine and Gaussian processes (GP).	RMSE = 21.4(40.5) Mg/ha

estimation at the individual tree level is promising, there are several limitations: (1) for small footprint LiDAR, the laser pulse may miss the tree top. Therefore, to accurately extract individual trees, point density is an important factor. Previous studies have shown that a point density lower than 4 m^{-2} might be insufficient for the identification of individual trees;[59,69,71] (2) in CHM applications, crown overlapping was the major issue for tree crown identification; (3) individual tree level methods were usually tedious, time consuming, and expensive for field data collection and validation; (4) subdominant trees could not be detected using LiDAR returns data, and the aggregation of individual trees within a plot underestimated the entire plot biomass; and (5) in mixed forest such as tropical forest, it would be difficult to acquire enough species-allometric. The individual tree level methods for biomass estimation could be greatly improved by fusion with spectral data to classify tree species. It is difficult to identify tree species using LiDAR data alone because there are no published standards for radiometric calibration of LiDAR intensity data. Few studies have showed classification of tree species using LiDAR intensity data alone. Donoghue et al.[72] studied tree species classification using LiDAR intensity data, but only two species were included in the study area. Even with the disadvantages listed above, this method could be greatly improved by fusion with other spectral remote sense data to identify tree species. Many studies have already illustrated the combined performance of LiDAR-derived parameters and spectral data for forest biomass estimation.[73–75] Furthermore, an adaptable model and LiDAR-derived parameters is needed to automatically identify trees and then calculate the forest biomass based on tree height.[63,68–70,76,77]

3.2 *Plot Level*

When the scope of the study is the plot, regression models were always used for forest biomass estimation based on LiDAR-derived statistics, such as height and canopy density metrics. Regression models usually use a simple/multiple and stepwise linear regression.[15,69,78] One of the pioneering studies is Nelson et al.[58] using two logarithmic equations in conjunction with six LiDAR-derived canopy measurements to estimate canopy volume and biomass. The model that used the mean plot height metric derived from all LiDAR pluses as an input parameter was identified as the best model. Previous studies indicated that tree height and crown diameter were highly correlated with biomass.[63,79] Some recent studies focused on canopy height metrics that take into account structural data at multiple heights throughout the whole forest canopy,[76] such as quadratic mean canopy height, height of median energy (HOME), height/median ratio (HTRT), simple ground return ratio (GRND), CH0.5-1.5 (as the proportion of laser hits above 0.5 m that belong to the height interval of 0.5–1.5 m), CH1.5-2.5, CH2.5-3.5, and CH3.5-4.5.[71] Lefsky et al.[78] employed simple linear models involving the parameters of maximum canopy height, median canopy height, mean canopy eight, and quadratic mean canopy height and found that these parameters account for 80%, 70%, 73% and 80% of the variation in the ABG estimation, respectively. Drake et al.[61] derived four metrics from LiDAR data: LiDAR canopy height, HOME, HTRT and a GRND. The four metrics were then input into a stepwise regression procedure to predict field-estimated AGB with r^2 (correlation coefficient) up to 0.93. Means et al.[59] and Lefsky et al.[78] employed almost the same data processing and analysis techniques to demonstrate the capabilities of Scanning LiDAR Imager of Canopies by Echo Recovery (SLICER) for AGB. Means et al.[59] concluded that models using (1) mean canopy height, (2) quadratic mean canopy height and mean canopy height, and (3) the sum of the portion of waveform return from the canopy as predictors account for 90%, 94%, and 96% of variation in AGB estimation. Riggins et al.[76] calculated multiple height percentiles (5, 15, 25, 35, 45, 55, 65, 75, 85, 95 and 100th percentiles) from small-footprint aerial LiDAR data and used a regression-tree model to get the forest biomass. Lefsky et al.[80] applied a single regression including the parameters of LiDAR measured canopy structure in three different biomes and explained that these parameters account for 84% of the variance in AGB estimation ($P < 0.0001$). Lim and Treitz[81] introduced quartile estimators (at 0, 25, 50, 75 and 100th percentiles) derived from airborne discrete return laser scanner data to estimate forest AGB. The coefficient of determination (r^2) for each model was >0.8. Zhao et al.[64] proposed a scale-invariant forest biomass estimation method and obtained promising results. Rowell et al.[82] estimated conifer-mixed forest biomass using both generalized and species-specific allometric models.

As far as data analysis is concerned, a wide variety of machine learning models have been effectively used in forest applications such as ANN,[42] support vector regressions (SVRs),[65,67] random forest (RF),[67] cubist,[83] bagging,[83] and various algorithms based on decision trees (DTs) such as single and ensemble regression trees.[71] Van Aardt et al.[84] assessed a LiDAR-based, object-oriented approach to forest AGB models. The results showed that the new method was better than previous stand-based and plot-based approaches. Zhao et al.[65] used two kernel machines, a support vector machine (SVM), and Gaussian processes to relate canopy characteristics to high-dimensional LiDAR metrics. Results illustrated that two machine learning models in conjunction with LiDAR metrics outperformed traditional approaches such as maximum likelihood classifier (MLC) and linear regression models. Gleason and Im[67] used machine learning approaches to estimate forest biomass. In their study, four modeling techniques were used for moderately dense forest biomass estimation, including linear mixed effects regression, RF, SVR, and cubist. Results indicated that when estimating biomass at the plot level, the SVR modeling technique produced the most accurate biomass, whereas at the individual tree level, similar results were obtained by all models. The relationship between crown identification accuracy and biomass estimation accuracy is complex and needs to be further investigated. Figure 2 is a diagram summarizing some existing methods for biomass estimation using LiDAR data.

The space-borne full-wave laser system Ice, Cloud, and land Elevation satellite (ICESat)/geoscience laser altimeter system (GLAS) has been used to estimate vegetation height[85–87] and forest biomass in large areas of the globe.[73,88,89] These studies were mainly based on waveform decomposition. Duncanson et al.[87] estimated forest canopy height from GLAS waveform

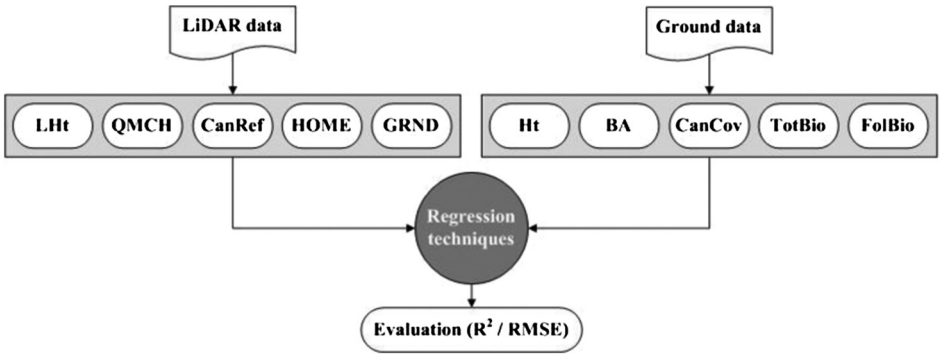

Fig. 2 Process of biomass estimation by LiDAR data (LHt: mean canopy height derived from LiDAR data; QMCH: quadratic mean canopy height; CanRef: canopy reflection sum; HOME: height of median energy; GRND: a simple ground return ratio; Ht: mean canopy height; BA: basal area; CanCov: canopy cover (range 0 to 1); TotBio: total above ground stand biomass; FolBio: foliage biomass).

metrics. Results indicated that GLAS waveforms could estimate forest height and AGB accurately, especially in flat areas with homogeneous forest conditions. Sun et al.[86] also demonstrated that the vertical information derived from the GLAS waveform was very similar to that of the laser vegetation imaging sensor (LVIS) waveform which has been successfully used for forest structural parameters estimation. Although there are many studies on sub-boreal forest systems using ICESat/GLAS data, hardly any research exists on temperate, dry or tropical forests. This was mainly due to the sparse sampling density. Additionally, ICESat/GLAS data were often integrated with imaging sensors.[34,88] Boudreau et al.[88] combined multiple data sources to estimate biomass, including GLAS, SRTM, Landsat ETM+, airborne LiDAR, ground inventory plots, and vegetation zone maps. Their study showed that space-borne remote sensing measurements could be efficiently used for biomass estimation over large areas.

Increasingly, more studies focus on the detection of change in the AGB. By correlating LiDAR to forest inventory data, Jubanski et al.[90] attempted to estimate AGB and its variability across large areas of tropical lowland forests. Huang et al.[91] used NASA's Laser Vegetation Imaging Sensor data for mapping biomass change. Meyer et al.[92] also researched detecting tropical forest biomass dynamics from repeat LiDAR measurements. Næsset et al.[93] detected change of forest biomass over an 11-year period using airborne LiDAR data. Englhart et al.[94] quantified changes of tropical peat swamp forest with multitemporal LiDAR datasets. In the future, the fusion of LiDAR with other sensors is the tendency for biomass estimation. He[95] fused LiDAR with SPOT-5 data to estimate coniferous forest biomass. Tsui et al.[96] conducted a study to fuse multifrequency radar and discrete-return LiDAR measurements for AGB estimation in a costal temperate forest. Tsui et al.[97] focused on the fusion of LiDAR and radar for forest biomass estimation.

4 AGB Estimation with Hyperspectral Data

Hyperspectral imagery can provide numerous narrow bands. Compared with traditional multispectral imagery, hyperspectral can separate subtle changes of the biophysical parameters of forest.[98] Because of this strength, hyperspectral imagery has been used for classifying vegetation species,[23,99,100–108] extracting tree health information,[109,110] deriving biophysical parameters,[26,109,111,112] and estimating biomass.[110] Pu and Gong[112] used EO-1 Hyperion data to map forest crown closure (CC) and leaf area index (LAI). Three methods were used in their study, including: band selection, principal component analysis (PCA), and wavelet transform (WT). Results show that WT was the most effective method for mapping forest CC and LAI (mapping accuracy for CC = 84.9%, LAIMA = 75.39%). Zhang et al.[109] explored a process-based method to retrieve leaf chlorophyll content from hyperspectral remote sensing imagery in complex forest canopies. Dalponte et al.[107] evaluated two high spectral and spatial resolution hyperspectral sensors for tree species classification, where SVM, RF, and Gaussian maximum likelihood (ML) classification methods were used. Their results suggest that there was no

significant difference between SVM and RF classifiers and that the image spatial resolution had a strong effect on the classification accuracy.

Hyperspectral remote sensing data such as MODIS, Hyperion, AVHRR, AISA, HyMap, AVIRIS, and DAIS have also been frequently used for quantifying biomass from local to global scales.[74,113–116] Among them, the spatial resolutions of MODIS and AVHRR are 250 m to 1 km and 1.1 km, respectively, and are usually used for forest biomass estimation at a regional or global scale. Dong et al.[117] utilized normalized difference vegetation index (NDVI) derived from AVHRR images for forest biomass estimation. Because MODIS is a hyperspectral sensor, numerous band and index combinations can be used for regression modeling. At regional and global scales, MODIS and AVHRR are promising for forest biomass estimation. However, there are two major limitations of these sensors for forest biomass study: (1) because of low spatial resolution, it was not appropriate for small-area forest research; (2) because of long lapses, it was difficult to avoid the influence of cloud cover, especially the missing information of interesting areas.[12] To make up for these limitations, fusion with other sensors might provide more accurate results in forest biomass estimation, especially the combination of spectral information and structural information.

For airborne hyperspectral sensors, most of the existing studies utilized different ways for forest biomass estimation, including raw spectral bands,[99,100] regression analysis,[115] and machine learning methods such as SVMs,[104] end-member methods,[108,118,119] ML classification, spectral angle mapper (SAM), RF, genetic algorithms, regression trees, ANN, and DT classifiers.[107] Hansen and Schjoerring[115] used NDVI in a linear regression analysis for estimating green biomass. The results showed that partial least square regression analysis may provide a useful tool when applied to hyperspectral data. Dong et al.[117] used a multiple linear regression analysis to investigate the relationship between field estimates of AGB and various vegetation indices (VIs) acquired by hyperspectral data. Cho et al.[116] used spectral indices and partial least squares regression to estimate green grass/herb biomass in a seminature landscape from airborne hyperspectral imagery. Their results showed that partial least squares regression combined with airborne hyperspectral imagery provides a better result than unvaried regression involving hyperspectral indices for grass/herb biomass estimation in Majella National Park, Italy. Gong et al.[120] utilized Airborne Imaging Spectrometer Applications (AISA) hyperspectral imagery for forest biomass estimations for three forest crops. In their study, VIs and red edge positions (REPs) were derived from hyperspectral imagery and then regression models were used for the estimation of forest biomass. Results indicated that both VIs and REPs were effective for forest biomass estimation.

Some studies argued that a direct estimation of AGB cannot be achieved from hyperspectral imagery alone due to the weak relationship between vegetation biomass and spectral indices,[121] especially in dense forests. However, it seems that fusion of hyperspectral and other types of remotely sensed data for biomass estimation is a promising area that needs further investigation.

5 AGB Estimation with Fusion of Hyperspectral and LiDAR Data

As no single data type could fulfill all requirements in AGB estimation, the complementary information of the fused data has obtained increasing interest. For tree-level biomass estimation, the species type is needed for application of species-specific allometric equations. Compared with multispectral data, hyperspectral data have shown to be promising in species classification[101] and spectral attributes.[21] Therefore, species classification maps derived from hyperspectral data could be used as an additional parameter to refine models based on LiDAR-derived metrics and intensity information. To date, many studies have been focused on the fusion of hyperspectral and LiDAR data for a variety of applications, including crown identification,[23] AGB estimation,[74] sagebrush distribution mapping,[122] and fuel type mapping.[123] Furthermore, numerous studies have particularly investigated forest species classification,[23,104,106,124–126,127,128] vegetation type classification,[100] and species-level discrimination.[23,74,128] Additionally, the LiDAR/hyperspectral fusion has also been shown to increase the capacity of image segmentation and object-based classification.[100,128]

Although numerous previous studies used the fusion of hyperspectral and LiDAR data in forest applications, most of the studies focused on forest species classification. For the fusion of hyperspectral and LiDAR data, there were three general levels as introduced in Sec. 2.4: pixel-level fusion, feature-level fusion, and decision-level fusion. Most of the existing studies used pixel-level fusion, which includes the following major steps: (1) preprocessing of hyperspectral and LiDAR data; (2) creating a combined dataset; (3) applying machine learning methods for forest species classification, such as SVM,[129] RF,[106,125] object-based classification,[127] and Gaussian ML.[103] Hill and Thomson[100] fused Hymap images and airborne LiDAR data on the pixel level to classify woodland species. In their study, a digital canopy height model and the first two principal components from HyMap data were processed by a parcel-based unsupervised classification approach. Naidoo et al.[106] also conducted an experiment to accurately classify and map individual trees at the species level in a savanna ecosystem. Hyperspectral- and LiDAR-derived parameters were grouped into seven predictor datasets and then an automated RF modeling approach was applied to classify eight common savanna tree species in the Greater Kruger National Park region, South Africa. The results showed that the most significant predictors were the NDVI, the chlorophyll b wavelength (chlorophyll includes chlorophyll a, chlorophyll b, chlorophyll c, chlorophyll d, and chlorophyll f. The range of chlorophyll b absorption wavelength is from 460 to 645 nm) and a selection of raw, continuum removed and SAM bands. Naidoo et al.[106] also concluded that RF modeling with hybrid datasets yielded the highest accuracy for the eight tree species with an overall accuracy of 87.68%. There are other classification methods for information extraction from LiDAR–hyperspectral datasets, for example, object-oriented classification methods,[127] RF classifier,[125] SVM, and Gaussian ML.[103] Feature-level fusion is a little different from pixel-level fusion. The major differences between them are in step (2) and step (3). In feature-level fusion, step (2) is used to derive LiDAR and hyperspectral metrics, such as canopy height and NDVI, and step (3) is used to form the combined dataset (combination of LiDAR and hyperspectral-derived metrics). Puttonen et al.[129] used datasets consisting of two reflectance and two shape parameters to classify coniferous and deciduous trees and individual tree species through a SVM method, and the best classification result was 95.8% for the separation of coniferous and deciduous trees. Dalponte et al.[125] extracted LiDAR (i.e., H_{min}, H_{max}) and hyperspectral metrics, respectively, and then a feature-selection technique was used to extract variables that have the most information. Several fused bands were formed including all hyperspectral bands, spectral bands + max height (LiDAR low density), spectral bands + max height (LiDAR high density), and spectral bands + height features (LiDAR height density). A nonlinear SVM and an RF classifier were used to classify tree species. When combined with either hyperspectral or multispectral data, high-density LiDAR data could provide more information for tree species than low density LiDAR data. As few studies used decision-level fusion of multiple data, decision-level fusion will not be discussed here. Figure 3 shows the preprocessing of LiDAR and hyperspectral data before fusion. Figure 4 illustrates the pixel-level fusion of hyperspectral and LiDAR for forest species distribution mapping. Table 2 shows the previous studies of forest biomass estimation using the fusion of hyperspectral and LiDAR data.

In addition to species classification, hyperspectral and LiDAR fusion data were also used for forest biomass estimation. Hyperspectral sensors were used for species classification, and then LiDAR data were used to perform biomass estimation of each classified species. The fusion of LiDAR and hyperspectral data included the following steps: (1) preprocessing of each

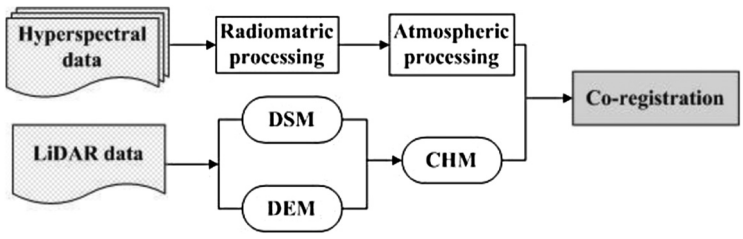

Fig. 3 Preprocessing of LiDAR and hyperspectral data.

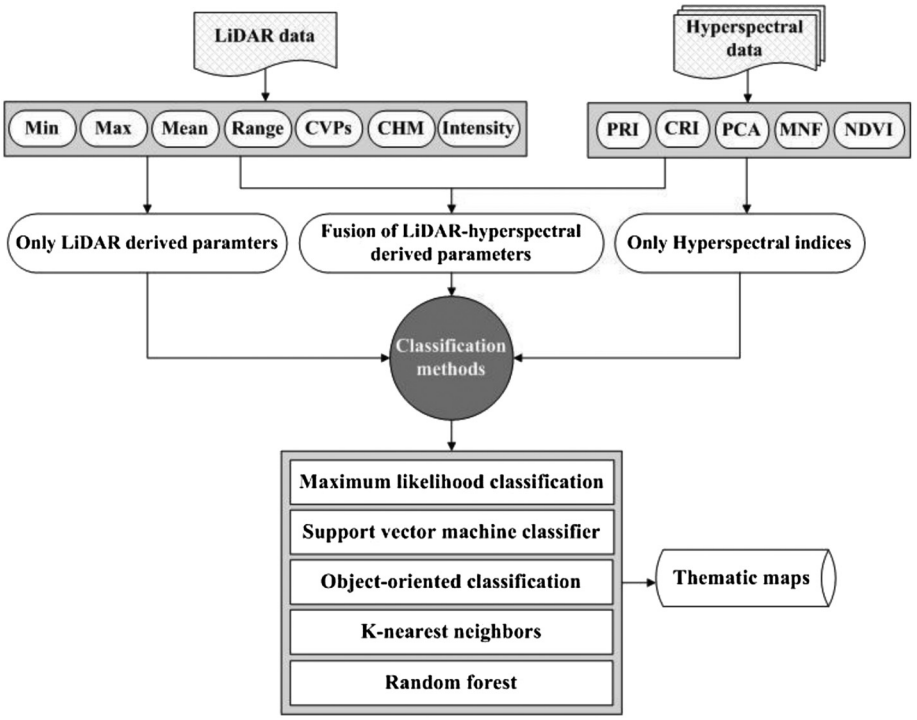

Fig. 4 Pixel-level fusion of hyperspectral and LiDAR for forest species distribution mapping, CVPs: canopy volume profiles; PRI: photochemical reflectance index; CRI: carotenoid reflectance index; PCA: principal component analysis; MNF: minimum noise fraction; NDVI: normalized difference vegetation index.

data (i.e., removing clear outlier points from LiDAR data, atmospheric correction of hyperspectral data, co-register LiDAR and hyperspectral data); (2) deriving LiDAR and hyperspectral metrics (e.g., canopy height model from LiDAR data, height metrics from CHM, varieties of vegetation index); (3) classifying forest species using hyperspectral data and creating the combined dataset; and (4) estimating forest biomass using regression methods or a species-specific allometric. In a complex forest, Lucas[74] used airborne LiDAR data and CASI hyperspectral image data to automatically identify trees and estimate their biomass. In their study, a Jackknife linear regression was also used to estimate plot-level forest biomass using six LiDAR strata heights and crown cover. Results showed that the Jackknife linear regression method was more robust for forest biomass estimation and showed a closer relationship with plot-sale ground data ($r^2 = 0.90$, RSE $= 11.8$ Mg/ha, $n = 31$). The fusion study also required methods which could deal with high-density LiDAR data and complex forests. Clark et al.[8] estimated tropical forest biomass using the fusion of hyperspectral and small-footprint, discrete-return LiDAR data. LiDAR metrics (i.e., mean height, maximum height) and hyperspectral metrics (i.e., NDVI) were retrieved, respectively. Then single and two-variable linear regression analyses were used to relate plot-scale LiDAR and hyperspectral metrics to field-derived biomass from all plots. The results showed that the best model was created using all 83 biomass plots including two LiDAR height metrics, plot-level mean height, and maximum height with an r^2 of 0.90 and RMSE of 38.3 Mg/ha. However, analysis combined for plantation plots had the most accuracy field data with r^2 increased to 0.96 and RMSE of 10.8 Mg/ha ($n = 32$). Swatantran et al.[25] used LVIS metrics, AVIRIS spectral indices, multiple endmember spectral mixture analysis fraction, and linear and stepwise regressions to map species-specific biomass and stress at landscape scale. The results showed that the accuracy of prediction by LVIS after species stratification of the field data was up to $r^2 = 0.77$, and RMSE $= 70.12$ Mg/ha. The results also suggest that LiDAR data were better for biomass estimation, whereas the hyperspectral data were used to adjust the LiDAR predictive models for species. Latifi et al.[132] fused LiDAR-hyperspectral data for forest structure modeling, including models of stem density and aboveground total biomass. Their results indicated that LiDAR

Table 2 List of references on the fusion of hyperspectral/LiDAR for biomass estimation and forest species classification.

References	Parameters	Methods	Goals
Hill et al.[100]	PCs 1 and 2 of HyMap and Digital Canopy Height Model (DCHM)	Segmentation and ISODATA	Mapping of woodland species composition and structure
Geerling et al.[51]	Pixel-level fusion of 10 CASI bands and 6 LiDAR texture bands (min, max, mean, median, SD, and range)	MLC	Classification of floodplain vegetation
Sugumaran et al.[127]	4 band Quickbird image with and without LiDAR; 24-band AISA hyperspectral image with and without LiDAR; 63-band AISA Eagle hyperspectral image with and without LiDAR.	Object-oriented classification	Tree species identification in an urban environment
Dalponte et al.[103]	25 hyperspectral bands, elevation and intensity of the first LiDAR return; 40 hyperspectral bands, elevation and intensity of the first LiDAR return; 126 hyperspectral bands, elevation and intensity of the first LiDAR return.	SVM classifier; GML-LOOC; K-NN	Classification of complex forest
Jones et al.[104]	AISA data (40 bands); 40 AISA bands and CHM; 40 AISA bands and 4 CVPs; 40 AISA bands, and 2 CVPs	A multiclass SVM classifier	Mapping species distribution
Onojeghuo et al.[130]	Spectral data only; spectrally compressed data: PCA transformed data and MNF transformed data; SSPCA transformed data; texture combined data: MNF 1-15-GLCM45; (Optical MNF + texture) and LiDAR derived measures; Optical SSPCA image and LiDAR derived measures.	Maximum likelihood classifier (MLC)	Optimize the use of LiDAR and hyperspectral data for reedbed habitats mapping
Naidoo et al.[106]	Height only dataset; Hyperspectral indices only dataset (CRI, NDVI, PRI, red edge NDVI); Height and indices dataset (Height, CRI, NDVI, PRI, red edge NDVI); Raw bands datasets (all 72 CAO raw bands); SAM selected bands dataset (Band Add-On); Nutrient and Leaf Mass Bands Dataset	Random forest module	Classification of savanna tree species
Anderson et al.[131]	24 AVIRIS MNF bands and 4 LVIS metrics (RH25, RH75, RH50 and RH 100)	Stepwise mixed linear regression techniques	LiDAR-hyperspectral fusion for inventory of a northern temperate forest

Note: CVPs, canopy volume profiles; PRI, photochemical reflectance index; CRI, carotenoid reflectance index.

provided most of the information for the combination, whereas hyperspectral data only made a modest contribution. Figure 5 shows two methods of AGB estimation by fusion of LiDAR-hyperspectral dataset.

The above studies showed good results of data fusion for forest biomass estimation, yet there are still many aspects which need refinement for improving biomass estimation through fusion of hyperspectral and LiDAR data. The major limitations are: (1) a very high LiDAR sampling rate is required to correctly identify treetops;[133,134] (2) forest biomass estimation was affected by the plot size for some sensors; (3) at the individual tree level, if the spatial resolution is coarser than that of individual crown areas, it would be difficult to identify individual trees, especially in complex forests; and (4) in complex forests, subcanopy trees and stems are usually omitted from the traditional canopy height models, which would underestimate the biomass.

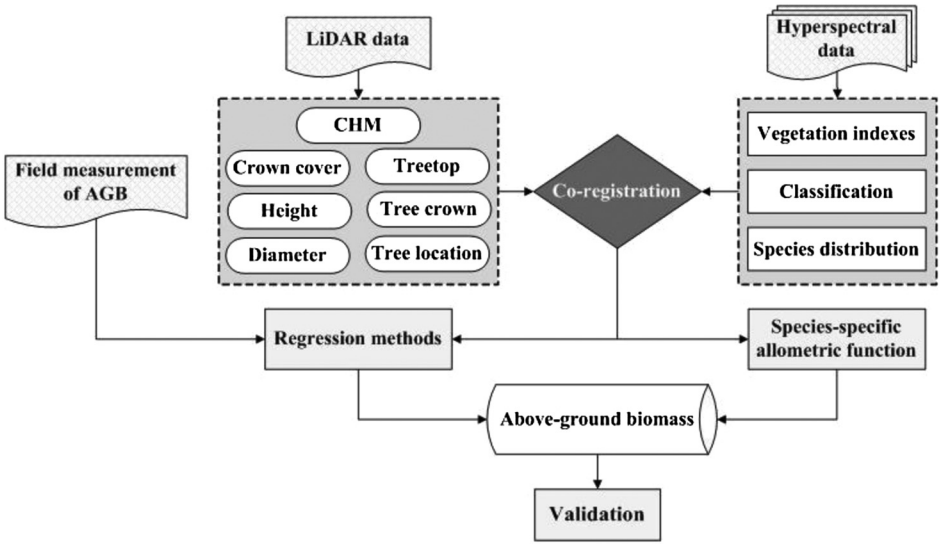

Fig. 5 Two methods of above-ground biomass (AGB) estimation by fusion of LiDAR-hyperspectral dataset.

6 Challenges and Future Research

LiDAR provides precise height information which could extract vertical and horizontal information of the forest[135] and is less sensitive to saturation when compared with other sensors. Hyperspectral data can provide detailed spectral information which can be used to effectively classify forest species. The findings on forest biomass estimation in the last decades are encouraging, and there is a growing interest for hyperspectral, LiDAR, and fusion of LiDAR and hyperspectral data for forest biomass estimation. However, there are still many limitations that should taken into account: (1) because a forest is a complex ecosystem, many factors may impact the estimation of forest biomass when using LiDAR and hyperspectral imagery, such as spectral and spatial resolution, co-registration of data from different sources (data from different platforms, different dates or with different resolutions), LiDAR point density, fusion framework, classification algorithm, allometric equations, plot-size, study area, stem density, canopy volume, and height; (2) although the Global Climate Observing System has suggested some accuracy levels, there is still no clear standard for forest biomass estimation. In addition, it is still unclear as to how forest biophysical and biochemical attributes derived from hyperspectral data relate to structural attributes from LiDAR data. The current methods normally add LiDAR elevation information as an extra band of hyperspectral data on the pixel level, or extract metrics, respectively, and classify fused images using different algorithms. In some other studies, hyperspectral and LiDAR data were processed separately. For example, hyperspectral data were used to classify forest species, and LiDAR data were used to identify individual trees, then specific allometric equations were used for forest biomass; (3) it is difficult to estimate forest biomass in forest with complex structures, especially tropical forests. In addition, high-quality ground truth data for validation is still lacking. For example, it is unrealistic to classify all tree species with hyperspectral data[101] and classify all species-specific allometric equations; (4) for tree-level biomass estimation, although hyperspectral and LiDAR data have been successfully used, it is still problematic, because it is difficult to allocate individual trees to the proper species. Using a spatial resolution coarser than that of individual tree crown size, it is difficult to classify and attribute individual trees. In this case, tone can assume that there are several species within a pixel area, especially in heterogeneous forests. Using a spatial resolution finer than that of individual tree crown size, it is also difficult to classify and attribute individual trees. As in this case, an individual crown may contain several pixels with different illumination.

Although there are limitations as described above, the fusion of hyperspectral and LiDAR is still promising for forest biomass estimation, especially with the emergence of new sensors and new fusion methods.

6.1 *New Sensors*

Many dedicated missions will be launched.[136,137] For example, forthcoming hyperspectral missions will also be oriented toward image fusion, such as Environmental Mapping and Analysis Program (EnMap), PRecursore IperSpettrale of the application mission (PRISMA), Medium Resolution Imaging Spectrometer (MERIS), and Hyperspectral Infrared Imager (HyspIRI). A new processing and fusion framework will also need to deal with these new sensors.

6.2 *New Fusion Methods*

More advanced modeling methods are needed to quantify the biophysical characteristics of forest.[120] Compared with pixel-level classification, an object-based classification method is more accurate when segmenting tree crown.[74,138–140] Therefore, it is a reasonable step to implement simple crown segmentation algorithms to generate crown objects for future analysis, especially in a low density forest. However, the selection of optimal parameters remains a challenge in the case of a high-density forest area. The new fusion methods include the fusion of different sensors and the fusion of different modeling methods: (1) fusion of different sensors, including electro-optical, radar and LiDAR sensors; (2) fusion of direct and indirect methods. For example, biomass extracted from high resolution remotely sensed images over some study areas can be used in the less computationally demanding indirect regression methods; and (3) fusion of different modeling methods, such as SVM, RF, and object-based classification. The combination of these methods might improve the classification accuracy.

There are several questions that need further investigation: (1) can alteration in the fusion framework (pixel-level, feature-level and decision-level) of hyperspectral and LiDAR data lead to different findings? (2) Can feature selection methods be further improved to increase the stability and accuracy of tree species classification from hyperspectral data? (3) Can additional LiDAR measures be connected to forest structure and canopy architecture?

7 Conclusions

In this paper, the application of LiDAR data, hyperspectral data, and LiDAR/hyperspectral data fusion for forest biomass estimation and the current difficulties and prospects were reviewed. Generally, using remote sensing data, forest biomass could be directly estimated with different methods, including multiple regression analysis, *K* nearest-neighbor and neural network. Forest biomass could also be indirectly estimated. For example, canopy parameters such as crown diameter are derived from remotely sensed data and finally. allometric equations were used for forest biomass estimation.

Data from LiDAR systems such as ICESat/GLAS, SLICER, LVIS and discrete return LiDAR have been used for forest biomass estimation. Biomass estimation from airborne LiDAR metrics is more accurate than that from a satellite-borne GLAS instrument. The sparse sampling density of GLAS and the limited spatial extent of airborne LiDAR can be integrated with data from other imaging sensors. The methods of biomass estimation using LiDAR data include single regression between LiDAR-derived height metrics, tree crown delineation and biomass, stochastic simulation, and machine learning approaches. It is expected that more studies will focus on the variability of AGB estimated from LiDAR data and will multisensor measurements to estimate biomass, including LiDAR-radar fusion and LiDAR-hyperspectral fusion.

Hyperspectral data have been used for classifying vegetation species, monitoring health status, and deriving biophysical parameters. The main methods for information extraction from hyperspectral data include SVMs, ML, ANN, RF, DT, and end-member methods. Due to the loss of correlation, a few studies have used hyperspectral data for biomass estimation, especially in forests with high biomass and complex environmental conditions. Hyperspectral data fused with other types of remotely sensed data will be a promising research area for forest biomass estimation.

Since LiDAR data can characterize the vertical structure of forests with high accuracy and hyperspectral data can provide detailed spectral information on biophysical parameters, the fusion of LiDAR and hyperspectral data has received increased attention. There are three levels

of data fusion using LiDAR and hyperspectral data, including pixel level, feature level, and decision level. LiDAR/hyperspectral data fusion has been applied to AGB estimation and tree species classification. However, most of the studies were focused on forest species classification. As forest is a complex ecosystem, many factors may impact the estimation of forest biomass when using LiDAR and hyperspectral imagery, such as spectral and spatial resolution, co-registration of data from different sources (data from different platforms, different dates or with different resolutions), LiDAR point density, fusion framework, classification algorithm, allometric equations, plot-size, study area, stem density, canopy volume, and height. In addition, new systems which occupy complementary sensors on the same platform are emerging, such as Goddard's LiDAR, Hyperspectral and Thermal (GLiHT) airborne imager which shows promising prospects for the fusion of hyperspectral and LiDAR data.[141] In the near future, new satellite-based sensors will be launched, including the Medium Resolution Imaging Spectrometer (MERIS). These developments will provide more opportunities for multisensor fusion. Besides the fusion of hyperspectral-LiDAR data for forest biomass, there will be more fusions between multiple sensors and methods, including the fusion of different sensors (fusion of space-borne LiDAR, airborne LiDAR data, and hyperspectral data for upscaling forest biomass estimation), the fusion of direct and indirect methods for forest biomass (biomass extracted from high resolution remote sensing can be used in the less computationally demanding indirect regression methods), and the fusion of different machine learning methods.

Acknowledgments

This research was funded by the ABCC Program of the National Natural Science Foundation of China (Project 41120114001), and the National Key Technology R&D Program (Projects 2012BAC16B01 and 2012BAH27B05). The first author would like to thank the China Scholarship Council for the support of two years' study in the Department of Geography, University of North Texas. The authors would like to thank anonymous reviewers for their helpful comments and suggestions.

References

1. S. Brown and A. E. Lugo, "Aboveground biomass estimates for tropical moist forests of the Brazilian Amazon," *Interciencia* **17**(1), 8–18 (1992).
2. R. A. Houghton, "Aboveground forest biomass and the global carbon balance," *Global Change Biol.* **11**, 945–958 (2005).
3. B. Koch, "Status and future of laser scanning, synthetic aperture radar and hyperspectral remote sensing data for forest biomass assessment," *ISPRS J. Photogramm. Remote Sens.* **65**, 581–590 (2010).
4. M. Dalponte, L. Bruzzone, and D. Gianelle, "Fusion of hyperspectral and LiDAR remote sensing data for the estimation of tree stem diameters," in *Geoscience and Remote Sensing Symposium*, Vol. 2, pp. II-1008–II-1011 (2009).
5. A. Rosenqvist et al., "A review of remote sensing technology in support of the Kyoto Protocol," *Environ. Sci. Police* **6**, 441–435 (2003).
6. A. Angelsen et al., *Realizing REDD+ national strategy and policy options*, Center for International Forestry Research, Bogor, Indonesia (2009).
7. R. Defries et al., "Earth observations for estimating greenhouse gas emissions from deforestation in developing countries," *Environ. Sci. Policy* **10**, 385–394 (2007).
8. M. L. Clark et al., "Estimation of tropical rain forest aboveground biomass with small-footprint LiDAR and hyperspectral sensors," *Remote Sens. Environ.* **115**, 2931–2942 (2011).
9. S. Goetz and R. Dubayah, "Advances in remote sensing technology and implications for measuring and monitoring forest carbon stocks and change," *Carbon Manage.* **2**, 231–244 (2011).
10. R. K. Dixon et al., "Forest sector carbon offset projects: near-term opportunities to mitigate greenhouse gas emissions," *Water Air Soil Pollut.* **70**, 561–577 (1993).

11. M. García et al., "Estimating biomass carbon stocks for a Mediterranean forest in central Spain using LiDAR height and intensity data," *Remote Sens. Environ.* **114**, 816–830 (2010).
12. C. J. Gleason and J. Im, "A review of remote sensing of forest biomass and biofuel: options for small-area applications," *GISci. Remote Sens.* **48**(2), 141–170 (2011).
13. M. Nilsson, "Estimation of tree heights and stand volume using an airborne LiDAR system," *Remote Sens. Environ.* **56**(1), 1–7 (1996).
14. D. Lu, "The potential and challenge of remote sensing-based biomass estimation," *Int. J. Remote Sens.* **27**(7), 1297–1328 (2006).
15. P. Propastin, "Large-scale mapping of aboveground biomass of tropical rainforest in Sulawesi, Indonesia, using Landsat ETM+ and MODIS data," *GISci. Remote Sens.* **50**(6), 633–651 (2013).
16. D. Lu and Q. Weng, "Spectral mixture analysis of the urban landscape in Indianapolis with Landsat ETM+ imagery," *Photogramm. Eng. Remote Sens.* **70**(9), 1053–1062 (2004).
17. J. E. Nichol and M. R. Sarker, "Improved biomass estimation using the texture parameters of two high-resolution optical sensors," *IEEE Trans. Geosci. Remote Sens.* **49**(3), 930–948 (2011).
18. S. Eckert, "Improved forest biomass and carbon estimations using texture measures from WorldView-2 satellite data," *Remote Sens.* **4**(4), 810–829 (2012).
19. F. González-Alonso et al., "Forest biomass estimation through NDVI composites. The role of remotely sensed data to assess Spanish forests as carbon sinks," *Int. J. Remote Sens.* **27**(24), 5409–5415 (2006).
20. P. Muukkonen and J. Heiskanen, "Biomass estimation over a large area based on stand wise forest inventory data and ASTER and MODIS satellite data: a possibility to verify carbon inventories," *Remote Sens. Environ.* **107**, 617–624 (2007).
21. S. L. Ustin et al., "Using imaging spectroscopy to study ecosystem processes and properties," *BioScience* **54**(6), 523–534 (2004).
22. G. P. Asner et al., "Carnegie airborne observatory: in-flight fusion of hyperspectral imaging and waveform light detection and ranging for three-dimensional studies of ecosystems," *J. Appl. Remote Sens.* **1**, 013536 (2007).
23. G. P. Asner et al., "Invasive species detection in Hawaiian rainforests using airborne imaging spectroscopy and LiDAR," *Remote Sens. Environ.* **112**, 1942–1955 (2008).
24. B. Koetz et al., "Fusion of imaging spectrometer and LIDAR data over combined radiative transfer models for forest canopy characterization," *Remote Sens. Environ.* **106**, 449–459 (2007).
25. A. Swatantran et al., "Mapping biomass and stress in the Sierra Nevada using LiDAR and hyperspectral data fusion," *Remote Sens. Environ.* **115**, 2917–2930 (2011).
26. P. M. Treitz and P. J. Howarth, "Hyperspectral remote sensing for estimating biophysical parameters of forest ecosystems," *Progress in Phys. Geogr.* **23**, 359–390 (1999).
27. M. Govender, K. Chetty, and H. Bulcock, "A review of hyperspectral remote sensing and its application in vegetation and water resource studies," *Water Sa* **33**(2), 145–151 (2007).
28. E. Adam, O. Mutanga, and D. Rugege, "Multispectral and hyperspectral remote sensing for identification and mapping of wetland vegetation: a review," *Wetlands Ecol. Manage.* **18**, 281–296 (2010).
29. K. Lim et al., "LiDAR remote sensing of forest structure," *Prog. Phys. Geogr.* **27**, 88–106 (2003).
30. M. Van Leeuwen and M. Nieuwenhuis, "Retrieval of forest structural parameters using LiDAR remote sensing," *Eur. J. Forest Res.* **129**(4), 749–770 (2010).
31. S. Frolking et al., "Forest disturbance and recovery: a general review in the context of spaceborne remote sensing of impacts on aboveground biomass and canopy structure," *J. Geophys. Res.: Biogeosci (2005–2012)* **114**(G2), 1–27 (2009).
32. M. A. Wulder et al., "LiDAR sampling for large-area forest characterization: a review," *Remote Sens. Environ.* **121**, 196–209 (2012).
33. R. O. Dubayah and J. B. Drake, "LiDAR remote sensing for forestry," *J. Forestry*, **98**, 44–46 (2000).

34. S. G. Zolkos, S. J. Goetz, and R. Dubayah, "A meta-analysis of terrestrial aboveground biomass estimation using LiDAR remote sensing," *Remote Sens. Environ.* **128**, 289–298 (2013).
35. C. Vaiphasa, S. Ongsomwang, and T. Vaiphasa, "Tropical mangrove species discrimination using hyperspectral data: a laboratory study," *Estuarine Coast. Shelf Sci.* **65**, 371–379 (2005).
36. D. A. Clark et al., "Net primary production in tropical forests: an evaluation and synthesis of existing field data," *Ecol. Appl.* **11**, 371–384 (2001a).
37. D. A. Clark et al., "Measuring net primary production in forests: concepts and field methods," *Ecol. Appl.* **11**, 356–370 (2001b).
38. M. Keller, M. Palace, and G. Hurtt, "Biomass estimation in the Tapajos National Forest, Brazil Examination of sampling and allometric uncertainties," *Forest Ecol. Manage.* **154**, 371–382 (2001).
39. P. S. Roy and S. A. Ravan, "Biomass estimation using satellite remote sensing data-an investigation on possible approaches for natural forest," *J. Biosci.* **21**, 535–561 (1996).
40. R. F. Nelson et al., "Secondary forest age and tropical forest biomass estimation using Thematic Mapper imagery," *Bioscience* **50**, 419–431 (2000).
41. M. K. Steininger, "Satellite estimation of tropical secondary forest aboveground biomass data from Brazil and Bolivia," *Int. J. Remote Sens.* **21**, 1139–1157 (2000).
42. G. M. Foody, D. S. Boyd, and M. E. J. Cutler, "Predictive relations of tropical forest biomass from Landsat TM data and their transferability between regions," *Remote Sens. Environ.* **85**, 463–474 (2003).
43. D. Zheng et al., "Estimating aboveground biomass using Landsat 7 ETM+ data across a managed landscape in northern Wisconsin, USA," *Remote Sens. Environ.* **93**, 402–411 (2004).
44. Y. Wu and A. H. Strahler, "Remote estimation of crown size, stand density, and biomass on the Oregon transect," *Ecol. Appl.* **4**, 299–312 (1994).
45. C. E. Woodcock et al., "Inversion of the Li-Strahler canopy reflectance model for mapping forest structure," *IEEE Trans. Geosci. Remote Sens.* **35**, 405–414 (1997).
46. M. Phua and H. Saito, "Estimation of biomass of a mountainous tropical forest using Landsat TM data," *Can. J. Remote Sens.* **29**(4), 429–440 (2003).
47. S. C. Popescu, R. H. Wynne, and R. F. Nelson, "Measuring individual tree crown diameter with LiDAR and assessing its influence on estimating forest volume and biomass," *Can. J. Remote Sens.* **29**(5), 564–577 (2003).
48. D. G. Goodenough et al., "Comparison of AVIRIS and AISA airborne hyperspectral sensing for above-ground forest carbon mapping," in *IEEE Int. Geoscience and Remote Sensing Symposium*, Vol. 2, pp. II-129–II-132, IEEE (2008).
49. C. Pohl and J. L. Van Genderen, "Multi-sensor fusion: optimization and operationalization for mapping applications," *Proc. SPIE* **2232**, 17–25 (1994).
50. C. Pohl and J. L. Van Genderen, "Review article multi-sensor image fusion in remote sensing: concepts, methods and applications," *Int. J. Remote Sens.* **19**, 823–854 (1998).
51. G. W. Geerling et al., "Classification of floodplain vegetation by data fusion of spectral (CASI) and LiDAR data," *Int. J. Remote Sens.* **28**, 4263–4284 (2007).
52. M. Mangolini, "Apport de la fusion d'images satellitaires multicapteurs au niveau pixel en télédétection et photo-interprétation," Dissertation published at the University of Nice-Sophia Antipolis, France (1994).
53. E. Næsset, "Determination of mean tree height of forest stands using airborne laser scanner data," *ISPRS J. Photogramm. Remote Sens.* **52**, 49–56 (1997a).
54. S. Magnussen, E. Næsset, and T. Gobakken, "Reliability of LiDAR derived predictors of forest inventory attributes: a case study with Norway spruce," *Remote Sens. Environ.* **114**, 700–712 (2010).
55. H. O. Ørka, E. Næsset, and O. M. Bollandsås, "Classifying species of individual trees by intensity and structure features derived from airborne laser scanner data," *Remote Sens. Environ.* **113**, 1163–1174 (2009).
56. J. Hyyppä et al., "Forest inventory using small-footprint airborne LiDAR. Topographic laser ranging and scanning," in *Topographic Laser Ranging and Scanning: Principles and Processing*, pp. 335–370, CRC Press, Taylor & Francis (2009).

57. C. Mallet and F. Bretar, "Full-waveform topographic LiDAR: State-of-the-art," *ISPRS J. Photogramm. Remote Sens.* **64**, 1–16 (2009).
58. R. Nelson, W. Krabill, and J. Tonelli, "Estimating forest biomass and volume using airborne laser data," *Remote Sens. Environ.* **24**, 247–267 (1988).
59. J. E. Means et al., "Use of large-footprint scanning airborne LiDAR to estimate forest stand characteristics in the Western Cascades of Oregon," *Remote Sens. Environ.* **67**, 298–308 (1999).
60. M. A. Lefsky et al., "LiDAR remote sensing of above-ground biomass in three biomes," *Global Ecol. Biogeogr.* **11**(5), 393–399 (2002).
61. J. B. Drake et al., "Sensitivity of large-footprint LiDAR to canopy structure and biomass in a neotropical rainforest," *Remote Sens. Environ.* **81**, 378–392 (2002).
62. R. Nelson, A. Short, and M. Valenti, "Measuring biomass and carbon in Delaware using an airborne profiling LIDAR," *Scand. J. Forest Res.* **19**(6), 500–511 (2004).
63. S. C. Popescu, R. H. Wynne, and J. A. Scrivani, "Fusion of small-footprint LiDAR and multispectral data to estimate plot-level volume and biomass in deciduous and pine forests in Virginia, USA," *Forest Sci.* **50**(4), 551–565 (2004).
64. K. Zhao, S. Popescu, and R. Nelson, "LiDAR remote sensing of forest biomass: a scale-invariant estimation approach using airborne lasers," *Remote Sens. Environ.* **113**, 182–196 (2009).
65. K. Zhao et al., "Characterizing forest canopy structure with LiDAR composite metrics and machine learning," *Remote Sens. Environ.* **115**(8), 1978–1996 (2011).
66. R. F. Nelson et al., "Investigating RaDAR-LiDAR synergy in a North Carolina pine forest," *Remote Sens. Environ.* **110**(1), 98–108 (2007).
67. C. J. Gleason and J. Im, "Forest biomass estimation from airborne LiDAR data using machine learning approaches," *Remote Sens. Environ.* **125**, 80–91 (2012).
68. S. C. Popescu, "Estimating biomass of individual pine trees using airborne LiDAR," *Biomass Bioenergy* **31**, 646–655 (2007).
69. Z. J. Bortolot and R. H. Wynne, "Estimating forest biomass using small footprint LiDAR data: an individual tree-based approach that incorporates training data," *ISPRS J. Photogramm. Remote Sens.* **59**, 342–360 (2005).
70. D. Kwak et al., "Estimating stem volume and biomass of Pinus koraiensis using LiDAR data," *J. Plant Res.* **123**(4), 421–432 (2010).
71. J. Estornell et al., "Estimation of wood volume and height of olive tree plantations using airborne discrete-return LiDAR data," *GISci. Remote Sens.* **51**(1), 17–29 (2014).
72. D. N. M. Donoghue et al., "Remote sensing of species mixtures in Conifer plantations using LiDAR height and intensity data," *Remote Sens. Environ.* **110**(4), 509–522 (2007).
73. M. A. Lefsky et al., "Estimates of forest canopy height and aboveground biomass using ICESat," *Geophys. Res. Lett.* **32**(22), 1–4 (2005).
74. R. M. Lucas, A. C. Lee, and P. J. Bunting, "Retrieving forest biomass through integration of CASI and LiDAR data," *Int. J. Remote Sens.* **29**, 1553–1577 (2008).
75. T. Erdody and L. M. Moskal, "Fusion of LiDAR and imagery for estimating forest canopy fuels," *Remote Sens. Environ.* **114**, 725–737 (2010).
76. J. J. Riggins, J. A. Tullis, and F. M. Stephen, "Per-segment aboveground forest biomass estimation using LiDAR-derived height percentile statistics," *GISci. Remote Sens.* **46**(2), 232–248 (2009).
77. P. Gonzalez et al., "Forest carbon densities and uncertainties from LiDAR, quickbird, and field measurements in california," *Remote Sens. Environ.* **114**(7), 1561–1575 (2010).
78. M. A. Lefsky et al., "Surface LiDAR remote sensing of basal area and biomass in deciduous forests of eastern Maryland, USA," *Remote Sens. Environ.* **67**, 83–98 (1999).
79. E. Næsset and T. Økland, "Estimating tree height and tree crown properties using airborne scanning laser in a boreal nature reserve," *Remote Sens. Environ.* **79**(1), 105–115 (2002).
80. M. A. Lefsky et al., "LiDAR remote sensing for ecosystem studies," *Biosci.* **52**, 19–30 (2002).
81. K. S. Lim and P. M. Treitz, "Estimation of above ground forest biomass from airborne discrete return laser scanner data using canopy-based quantile estimators," *Scand. J. Forest Res.* **19**, 558–570 (2004).

82. E. Rowell et al., "Estimating plot-scale biomass in a western North America mixed-conifer forest from LiDAR-derived tree stems," in *Proc. SilviLaser Conf.*, pp. 14–16, Texas A&M University, College Station (2009).
83. M. Li et al., "Forest biomass and carbon stock quantification using airborne LiDAR data: a case study over Huntington wildlife forest in the Adirondack Park," *IEEE J. Sel. Top. Appl. Earth Obs. Remote Sens.* **7**(7), 3143–3156 (2014).
84. J. A. N. Van Aardt, R. H. Wynne, and R. G. Oderwald, "Forest volume and biomass estimation using small-footprint LiDAR-distributional parameters on a per-segment basis," *Forest Sci.* **52**(6), 636–649 (2006).
85. J. A. B. Rosette, R. R. J. North, and J. C. Suarez, "Vegetation height estimates for a mixed temperate forest using satellite laser altimetry," *Int. J. Remote Sens.* **29**(5), 1475–1493 (2008).
86. G. Sun et al., "Forest vertical structure from GLAS: An evaluation using LVIS and SRTM data," *Remote Sens. Environ.* **112**(1), 107–117 (2008).
87. L. I. Duncanson, K. O. Niemann, and M. A. Wulder, "Estimating forest canopy height and terrain relief from GLAS waveform metrics," *Remote Sens. Environ.* **114**(1), 138–154 (2010).
88. J. Boudreau et al., "Regional aboveground forest biomass using airborne and space borne LiDAR in Québec," *Remote Sens. Environ.* **112**(10), 3876–3890 (2008).
89. W. Huang et al., "Mapping forest aboveground biomass and its changes from LVIS waveform data," in *IEEE Int. Geoscience and Remote Sensing Symposium (IGARSS)*, pp. 6561–6564 (2012).
90. J. Jubanski et al., "Detection of large above-ground biomass variability in lowland forest ecosystems by airborne LiDAR," *Biogeosciences* **10**, 3917–3930 (2013).
91. W. Huang et al., "Mapping biomass change after forest disturbance: applying LiDAR footprint-derived models at key map scales," *Remote Sens. Environ.* **134**, 319–332 (2013).
92. V. Meyer et al., "Detecting tropical forest biomass dynamics from repeated airborne LiDAR measurements," *Biogeosci. Discuss.* **10**, 1957–1992 (2013).
93. E. Næsset et al., "Model-assisted estimation of change in forest biomass over an 11year period in a sample survey supported by airborne LiDAR: a case study with post-stratification to provide "activity data," *Remote Sens. Environ.* **128**, 299–314 (2013).
94. S. Englhart, J. Jubanski, and F. Sigegert, "Quantifying dynamics in tropical peat swamp forest biomass with multi-temporal LiDAR datasets," *Remote Sens.* **5**, 2368–2388 (2013).
95. Q. He, "Estimation of coniferous forest above-ground biomass using LiDAR and SPOT-5 data," in *2nd Int. Conf. IEEE Remote Sensing, Environment and Transportation Engineering (RSETE)*, pp. 1–4 (2012).
96. O. W. Tsui et al., "Using multi-frequency radar and discrete-return LiDAR measurements to estimate above-ground biomass and biomass components in a coastal temperate forest," *ISPRS J. Photogramm. Remote Sens.* **69**, 121–133 (2012).
97. O. W. Tsui et al., "Integrating airborne LiDAR and space-borne radar via multivariate kriging to estimate above-ground biomass," *Remote Sens. Environ.* **139**, 340–352 (2013).
98. J. Im and J. R. Jensen, "Hyperspectral remote sensing of vegetation," *Geogr. Compass* **2**(6), 1943–1961 (2008).
99. P. Bunting and R. Lucas, "The delineation of tree crowns in Australian mixed species forests using hyperspectral Compact Airborne Spectrographic Imager (CASI) data," *Remote Sens. Environ.* **101**(2), 230–248 (2006).
100. R. A. Hill and A. G. Thomson, "Mapping woodland species composition and structure using airborne spectral and LiDAR data," *Int. J. Remote Sens.* **26**, 3763–3779 (2005).
101. M. L. Clark, D. A. Roberts, and D. B. Clark, "Hyperspectral discrimination of tropical rain forest tree species at leaf to crown scales," *Remote Sens. Environ.* **96**, 375–398 (2005).
102. H. Buddenbaum, M. Schlerf, and J. Hill, "Classification of coniferous tree species and age classes using hyperspectral data and geostatistical methods," *Int. J. Remote Sens.* **26**, 5453–5465 (2005).
103. M. Dalponte, L. Bruzzone, and D. Gianelle, "Fusion of hyperspectral and LiDAR remote sensing data for classification of complex forest areas," *IEEE Trans. Geosci. Remote Sens.* **46**, 1416–1427 (2008).

104. T. G. Jones, N. C. Coops, and T. Sharma, "Assessing the utility of airborne hyperspectral and LiDAR data for species distribution mapping in the coastal Pacific Northwest, Canada," *Remote Sens. Environ.* **114**, 2841–2852 (2010).
105. J. Oldeland et al., "Mapping bush encroaching species by seasonal differences in hyperspectral imagery," *Remote Sens.* **2**, 1416–1438 (2010).
106. L. Naidoo et al., "Classification of savanna tree species, in the Greater Kruger National Park region, by integrating hyperspectral and LiDAR data in a Random Forest data mining environment," *ISPRS J. Photogramm. Remote Sens.* **69**, 167–179 (2012).
107. M. Dalponte et al., "Tree species classification in boreal forests with hyperspectral data," *IEEE Trans. Geosci. Remote Sens.* **51**(5), 2632–2645 (2013).
108. B. Somers and G. P. Asner, "Multi-temporal hyperspectral mixture analysis and feature selection for invasive species mapping in rainforests," *Remote Sens. Environ.* **136**, 14–27 (2013).
109. Y. Zhang et al., "Leaf chlorophyll content retrieval from airborne hyperspectral remote sensing imagery," *Remote Sens. Environ.* **112**, 3234–3247 (2008).
110. C. Wu et al., "Estimating chlorophyll content from hyperspectral vegetation indices: modeling and validation," *Agric. Forest Meteorol.* **148**, 1230–1241 (2008).
111. P. J. Zarco-Tejada et al., "Needle chlorophyll content estimation through model inversion using hyperspectral data from boreal conifer forest canopies," *Remote Sens. Environ.* **89**, 189–199 (2004).
112. R. Pu and P. Gong, "Wavelet transform applied to EO-1 hyperspectral data for forest LAI and crown closure mapping," *Remote Sens. Environ.* **91**, 212–224 (2004).
113. S. M. De Jong, E. J. Pebesma, and B. Lacaze, "Above-ground biomass assessment of Mediterranean forests using airborne imaging spectrometry: the DAIS Peyne experiment," *Int. J. Remote Sens.* **24**, 1505–1520 (2003).
114. M. A. Cho and A. K. Skidmore, "Hyperspectral predictors for monitoring biomass production in Mediterranean mountain grasslands: Majella National Park, Italy," *Int. J. Remote Sens.* **30**, 499–515 (2009).
115. P. M. Hansen and J. K. Schjoerring, "Reflectance measurement of canopy biomass and nitrogen status in wheat crops using normalized difference vegetation indices and partial least squares regression," *Remote Sens. Environ.* **86**, 542–553 (2003).
116. M. A. Cho et al., "Estimation of green grass/herb biomass from airborne hyperspectral imagery using spectral indices and partial least squares regression," *Int. J. Appl. Earth Obs. Geoinf.* **9**, 414–424 (2007).
117. J. Dong et al., "Remote sensing estimates of boreal and temperate forest woody biomass: carbon pools, sources, and sinks," *Remote Sens. Environ.* **84**(3), 393–410 (2003).
118. M. A. Cho et al., "Improving discrimination of savanna tree species through a multiple-endmember spectral angle mapper approach: Canopy-level analysis," *IEEE Trans. Geosci. Remote Sens.* **48**(11), 4133–4142 (2010).
119. A. Ghiyamat et al., "Hyperspectral discrimination of tree species with different classifications using single-and multiple-endmember," *Int. J. Appl. Earth Obs. Geoinf.* **23**, 177–191 (2013).
120. B. Gong et al., "Characterization of forest crops with a range of nutrient and water treatments using AISA hyperspectral imagery," *GISci. Remote Sens.* **49**(4), 463–491 (2012).
121. M. Schlerf and C. Atzberger, "Inversion of a forest reflectance model to estimate structural canopy variables from hyperspectral remote sensing data," *Remote Sens. Environ.* **100**, 281–294 (2006).
122. J. T. Mundt, D. R. Streutker, and N. F. Glenn, "Mapping sagebrush distribution using fusion of hyperspectral and LiDAR classifications," *Photogramm. Eng. Remote Sens.* **72**, 47 (2006).
123. B. Koetz et al., "Multi-source land cover classification for forest fire management based on imaging spectrometry and LiDAR data," *Forest Ecol. Manage.* **256**(3), 263–271 (2008).
124. J. Vauhkonen et al., "Classification of Spruce and Pine Trees Using Active Hyperspectral LiDAR," *IEEE Geosci. Remote Sens. Lett.* **10**, 1138–1141 (2013).

125. M. Dalponte, L. Bruzzone, and D. Gianelle, "Tree species classification in the Southern Alps based on the fusion of very high geometrical resolution multispectral/hyperspectral images and LiDAR data," *Remote Sens. Environ.* **123**, 258–270 (2012).
126. M. J. D. Sarrazin et al., "Fusing small-footprint waveform LiDAR and hyperspectral data for canopy-level species classification and herbaceous biomass modeling in savanna ecosystems," *Can. J. Remote Sens.* **37**(6), 653–665 (2011).
127. R. Sugumaran and M. Voss, "Object-oriented classification of LIDAR-fused hyperspectral imagery for tree species identification in an urban environment," in *Urban Remote Sensing Joint Event*, pp. 1–6, IEEE (2007).
128. M. Voss and R. Sugumaran, "Seasonal effect on tree species classification in an urban environment using hyperspectral data, LiDAR, and an object-oriented approach," *Sensors* **8**, 3020–3036 (2008).
129. E. Puttonen et al., "Tree classification with fused mobile laser scanning and hyperspectral data," *Sensors* **11**, 5158–5182 (2011).
130. A. O. Onojeghuo and G. A. Blackburn, "Optimizing the use of hyperspectral and LiDAR data for mapping reedbed habitats," *Remote Sens. Environ.* **115**, 2025–2034 (2011).
131. J. E. Anderson et al., "Integrating waveform LiDAR with hyperspectral imagery for inventory of a northern temperate forest," *Remote Sens. Environ.* **112**, 1856–1870 (2008).
132. H. Latifi, F. Fassnacht, and B. Koch, "Forest structure modeling with combined airborne hyperspectral and LiDAR data," *Remote Sens. Environ.* **121**, 10–25 (2012).
133. D. L. A. Gaveau and R. A. Hill, "Quantifying canopy height underestimation by laser pulse penetration in small-footprint airborne laser scanning data," *Can. J. Remote Sens.* **29**(5), 650–657 (2003).
134. J. L. Lovell et al., "Simulation study for finding optimal lidar acquisition parameters for forest height retrieval," *Forest Ecol. Manage.* **214**(1), 398–412 (2005).
135. S. J. Lee, J. R. Kim, and Y. S. Choi, "The extraction of forest CO2 storage capacity using high-resolution airborne LiDAR data," *GISci. Remote Sens.* **50**(2), 154–171 (2013).
136. G. V. Laurin et al., "Above ground biomass estimation in an African tropical forest with LiDAR and hyperspectral data," *ISPRS J. Photogramm. Remote Sens.* **89**, 49–58 (2014).
137. F. D. Van der Meer et al., "Multi-and hyperspectral geologic remote sensing: a review," *Int. J. Appl. Earth Obs. Geoinf.* **14**(1), 112–128 (2012).
138. A. Lobo, "Image segmentation and discriminant analysis for the identification of land cover units in ecology," *IEEE Trans. Geosci. Remote Sens.* **35**, 1136–1145 (1997).
139. C. Burnett and T. Blaschke, "A multi-scale segmentation/object relationship modelling methodology for landscape analysis," *Ecol. Model.* **168**, 233–249 (2003).
140. D. G. Leckie et al., "Automated tree recognition in old growth conifer stands with high resolution digital imagery," *Remote Sens. Environ.* **94**, 311–326 (2005).
141. B. D. Cook et al., "NASA Goddard's LiDAR, Hyperspectral and Thermal (G-LiHT) Airborne Imager," *Remote Sens.* **5**, 4045–4066 (2013).

Qixia Man is a PhD student at the East China Normal University. She studied at the University of North Texas as a visiting student from 2012 to 2014. Her research interests include digital image processing, LiDAR, and hyperspectral remote sensing.

Pinliang Dong is an associate professor in the Department of Geography, University of North Texas (UNT). He received his BSc degree from Peking University, China, MSc degree from the Institute of Remote Sensing Applications (IRSA), Chinese Academy of Sciences, and PhD degree from the University of New Brunswick, Fredericton, New Brunswick, Canada. His research interests are mainly in GIScience and remote sensing.

Huadong Guo is an academician and research professor at the Chinese Academy of Sciences. He graduated from the Geology Department at Nanjing University in 1977 and received his MSc degree from the Graduate University of the Chinese Academy of Science (CAS) in 1981. He is a guest professor of eight universities in China. His research interests include radar remote sensing, applications of Earth-observing technologies to global change, and Digital Earth.

Guang Liu received his BS/MS in physics from TsingHua University China in 1999/2002 and received his PhD degree from the Institute of Remote Sensing Applications of the CAS in 2008. He has been working with the Mathematic Geodesy and Positioning, Delft University of Technology of the Netherlands from 2006 to 2007 as a visiting researcher. He is an associate professor of Institute of Remote Sensing and Digital Earth, CAS. His work is focused on the study of the feasibility and potential applications of SAR image time series analysis.

Runhe Shi received his BS in East China Normal University in 2001, and received his PhD degree from Institute of Geographic Sciences and Natural Resources Research of the CAS. His research mainly focused on research and application of quantitative remote sensing algorithm.